

Investigation into Resonant Overvoltages in Wind Turbine Transformers due to Switching Surges

Cedric Amittai Banda and John Michael Van Coller

Abstract--This paper presents an investigation into resonant overvoltages in wind turbine transformers. The transformers are frequently switched by vacuum circuit breakers depending on the wind speed. Switching surges measured on-site which show repetitive, high du/dt transients were believed to contribute to the development of resonant overvoltages in the transformer windings. Two transformers with different core and winding arrangements but the same MV/LV voltage ratio and power rating were investigated. The transformers were rated 2.7 MVA, 0.690 / 33 kV with the MV side consisting of delta connected layer windings and the LV side consisting of star connected foil windings. A failed transformer had a wound core and used an egg-shaped winding whilst the special prototype transformer had a stacked core with split round windings. Part winding resonance tests carried out on one of the healthy windings of the failed transformer indicated a resonance amplification factor of 2.5 at 660 kHz. Measurements were also performed on the split winding prototype and results indicated that only the top half of the transformer coil had marked resonance effects. Calculations were then done using the Multi-Transmission Line model and results were verified against the measurements. The calculated and measured results had good agreement with the same profile from 1 kHz to 10 MHz.

Keywords: MTL model, resonant overvoltages, split winding design, switching surges and wind turbine transformer.

I. INTRODUCTION

Switching transients due to vacuum circuit breaker operation can lead to the development of resonant overvoltages in wind turbine transformers. In medium voltage networks the switching of vacuum circuit breakers [1], [2] can result in re-ignitions and pre-strikes. These high-frequency transients with high du/dt can lead to stressing of the end-turn insulation of the transformer. Resonance phenomena in transformer windings can be categorized as either internal resonance or external resonance. External resonance occurs due to cable and transformer interaction such that the natural frequency of the supplying cable matches the natural frequency of the transformer. This is more common in wind turbine

transformers where energization may result in cable transformer resonant transients [3]. Internal resonance occurs when the frequency of the incoming surge equals a resonant frequency of the transformer winding. These resonant overvoltages can result in a flashover from the windings to the core or between the turns [4]. However it should be noted that internal winding resonances will not necessarily result in immediate breakdown, but may result in partial discharges, which will further aid in insulation degradation and ultimately failure [1]. Transformer failure due to internal resonant overvoltages has been widely reported in [5], [6], and [7]. The increase in transformer dielectric failures led to the initiation of the CIGRE working group (A2/C4.39) and their findings were published in [8]. Although it was concluded that failures are mainly caused by the interaction of the transformer with the network for different cable lengths and loading conditions [9], [10], and [11] some of the expertise in transformer modelling will be applied in this paper. In [12], [13], and [14], the author investigated the frequency response of layer, pancake and disc winding types with the main focus being on resonant overvoltages in wind turbine transformers. A special prototype transformer with the three different winding designs was designed and manufactured. The results indicated that layer windings have a higher transferred overvoltage from LV to MV winding than disc and pancake windings. However the layer and pancake windings have a low voltage distribution further down in the middle of the winding and nearer to ground than the disc winding which keeps the high values of the voltage drops at resonant frequencies. This paper will focus on the layer type of winding with an interest on the resonant performance of split round windings. It should be noted that the analysis of very fast transients in layer-windings has been extensively researched in [4], [15], [16] and the use of the Multi-Transmission Line model for calculation of layer to layer voltage distribution will be used.

II. WOUND CORE TRANSFORMER

Failure of a wound core transformer on-site initiated the investigation into resonant overvoltages in wind turbine transformers and if switching surges could be a contributing factor. The damaged transformer when unwound at the transformer factory showed the inter-turn insulation was severely damaged as shown in Fig. 1. Substantial distortion of the first and second layer of the MV winding was also observed. A burn through the MV to LV barrier was also observed with a puncture through the first layer of the LV foil winding as shown in Fig. 2.

This work was funded by Eskom through the Eskom Power Plant Engineering Institute (EPPEI) program. C. A. Banda is currently with the University of Witwatersrand, Johannesburg, South Africa studying towards an MSc in Electrical Engineering (e-mail: cedric.banda@students.wits.ac.za). J. M. Van Coller is with the University of Witwatersrand and is a Senior Lecturer who has been with University for many years and holds the Eskom Chair of High Voltage (e-mail: john.vancoller@wits.ac.za).



Fig. 1. Failed winding with inter-turn insulation severely damaged.



Fig. 2. Burning of the first layer of the LV foil winding

Part winding resonance tests were conducted on one of the undamaged windings of the wound core transformer to ascertain if resonance could be a contributing factor to the damage observed in the transformer. A ratio known as the Resonance Voltage Ratio (RVR) was used which is defined as the voltage between points of resonance divided by the 50 Hz voltage at the same point. The method used was to excite the winding with a variable frequency sinusoidal voltage and record the maximum amplitude between two layers for a frequency range of 1 kHz to 2 MHz. The results are shown in Table I.

TABLE I
PART WINDING RESONANCE OF THE TRANSFORMER

Point in Winding	Frequency	RAF
Start of winding (between 2 layers)	536 kHz	1.15
Middle of winding (between 2 layers)	1.17 MHz	0.67
End of winding (between 2 layers)	181 kHz	0.95
End of winding (between 2 layers)	660 kHz	2.5
End of winding (between 2 layers)	1.32 MHz	0.67

From Table I at 660 kHz the amplification factor of 2.5 was recorded between the last and second last layer of the MV winding. This could result in a resonant overvoltage with a sufficient magnitude to stress the inter-turn insulation when closing transients occur. From Fig. 1, it is difficult to predict if the failure started as an inter-turn or inter-layer fault due to the burning of the oil paper insulation. However the failure

mechanism had sufficient magnitude to cause substantial distortion of the first two layers and create a puncture through to the LV foil winding. This paper will seek to address the above mentioned problem by investigating resonant performance of a split MV winding in comparison with the failed transformer that had a non-split MV winding through measurements and an analytical solution.

III. STACKED CORE PROTOTYPE TRANSFORMER

The design of the stacked core transformer is such that the inner winding is the LV winding whilst the outer winding is the MV winding. This differs from the wound core transformer as it had the MV winding sitting inside the LV winding with a static screen between the two windings. The wound core transformer used an egg-shaped winding against the stacked core's split round winding. The stacked core transformer prototype was installed with measuring taps at the end of each layer as shown in Fig. 3.

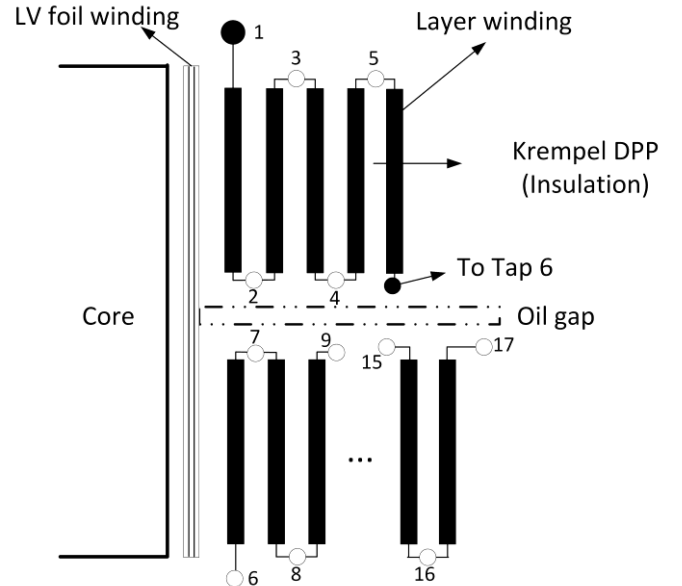


Fig. 3. Axisymmetric view of the prototype transformer

The upper coil consisted of 5 layers whilst the bottom coil consisted of 11 layers separated by an oil gap. It should be noted that both transformers had the same number of layers. The constructed prototype is shown in Fig. 4.

IV. ANALYTICAL MODEL OF THE TRANSFORMER

Analysis of the voltage distribution within the transformer windings can be represented by a group of interconnected and coupled transmission lines. The analytical modelling of the stacked core transformer was done using the Multi-Transmission Line (MTL) model. The MTL equations are described by (1) and (2):

$$\frac{d^2V}{dx^2} = -[Z][Y] \quad (1)$$

$$\frac{d^2I}{dx^2} = -[Z][Y] \quad (2)$$



Fig. 4. Prototype transformer with measuring taps installed.

where V and I are the incident voltage and current vectors respectively. Z and Y are the impedance and admittance matrices of the winding respectively. The solution of the above equation is well documented in [15] and [16] to yield Equation (3).

$$\begin{bmatrix} I_{S1} \\ 0 \\ \cdot \\ \cdot \\ 0 \\ 0 \end{bmatrix} = \begin{bmatrix} Y \end{bmatrix} \begin{bmatrix} V_{S1} \\ V_{S2} \\ \cdot \\ \cdot \\ V_{Sn} \\ V_{Rn} \end{bmatrix} \quad (3)$$

The matrix reduction techniques that are applied to get to equation (3) are best explained in [17]. Further manipulation of (3) results in (4). As the transformer winding is grounded $V_{Rn} = 0$ hence the last row can be removed as it is a redundant equation.

$$\begin{bmatrix} V_{S1} \\ V_{S2} \\ \cdot \\ \cdot \\ \cdot \\ V_{Sn} \end{bmatrix} = \begin{bmatrix} YY \end{bmatrix} \begin{bmatrix} I_{S1} \\ 0 \\ \cdot \\ \cdot \\ \cdot \\ 0 \end{bmatrix} \quad (4)$$

From (4), the voltages at the sending end of the winding between turn 2 and 1 are defined by: $V_{S1} = YY_{(1,1)} I_{S1}$ and $V_{S2} = YY_{(2,1)} I_{S1}$, hence the resonance voltage ratio is defined as:

$$H_1 = \frac{V_{S2}}{V_{S1}} = \frac{YY_{(2,1)}}{YY_{(1,1)}} \quad (5)$$

Equation (5) can be generalized to calculate the resonance voltage ratio at any arbitrary turn k as shown by (6)

$$H_k = \frac{V_{S(k+1)}}{V_{S1}} = \frac{YY_{(k+1,1)}}{YY_{(1,1)}} \quad k = 1, 2, \dots, n-1 \quad (6)$$

where YY is the inverse matrix of the matrix Y in (3). Equation (6) is the analytical expression of the RVR defined in section II and a comparison of the analytical calculation vs measured RVR is done in section VI.

V. DETERMINATION OF THE TRANSFORMER PARAMETERS

The impedance $Z = R + j\omega L$ and admittance $Y = G + j\omega C$ matrix of the MTL equations were calculated as shown in (7) and (8) from [5] and [6].

$$Z = \left[j\omega L + \left(\frac{1}{2(d_1 + d_2)} \right) \right] \sqrt{\frac{\pi f \mu}{\sigma}} \quad (7)$$

$$Y = (j\omega + \omega \tan \delta) \cdot C \quad (8)$$

where μ and σ are the permeability and conductivity of the conductor. d_1 and d_2 are the diameters of the conductors. In (7) the real part takes into account the skin effect at high frequencies [6]. The real part of (8) represents the dissipation factor ($\tan \delta$) or dielectric losses [15], [16]. It should be noted that $\tan \delta$ is frequency, moisture and temperature dependent and will influence the admittance matrix greatly at higher frequencies. An approximate equation for $\tan \delta$ shown in (9) was used to model the frequency dependency of the transformer insulation [3].

$$\tan(\delta) = (1.082 \times 10^{-8}) \cdot 2\pi f + 5.0 \times 10^{-3} \quad (9)$$

The capacitance and inductance matrix were calculated as follows:

A. Capacitance

The capacitance matrix C was formed as follows from [16]:

- Cii Capacitance of layer i to ground and the sum of all capacitances connected to layer i .
- Cij Capacitance between layers i and j taken with the negative sign ($i \neq j$)

The formulas for calculating the capacitance were calculated from the basic formulas of cylindrical and plate capacitors in [18] and are shown in (10), (11) and (12).

$$C_s = \frac{\epsilon_o \epsilon_r h}{d_s} \quad (10)$$

$$C_g = \frac{\epsilon_o \epsilon_r \omega}{d_g} \quad (11)$$

$$C_{ij} = \frac{2\pi\epsilon_o L}{\ln\left(\frac{b}{a}\right)} \quad (12)$$

where C_s is the turn to turn capacitance, C_g is the turn to earth capacitance and C_{ij} is the capacitance between layer i and j . ϵ_r is the relative permittivity of the dielectric material between the turns, ϵ_o is the permittivity of free space. h is the rectangular conductor's height. ds and dg are the distance between the turns and distance between turn and ground plane respectively. L is the length of the winding and w is the rectangular conductor's width. a and b are the inner and outer radius of the winding respectively.

The procedure for the construction of the capacitance matrix is explained in [19]. A matrix reduction technique explained in [20], [21] can be applied such that the order of matrices corresponds not to a single turn but to a group of turns. In this paper the group of turns will represent each layer of the MV winding.

B. Inductance

The inductance matrix is calculated from two parts. The first is directly from the capacitance matrix C if the following assumptions are made [17]:

1. High frequency magnetic flux penetration into the iron laminations and transformer core is negligible.
2. The magnetic flux will be constrained within the paths of the insulation.

The first inductance matrix can then be obtained using (13):

$$L_n = \frac{\epsilon_r}{v^2} \cdot C^{-1} \quad (13)$$

where v is the velocity of light in vacuum and ϵ_r is the relative permittivity of the insulation (in this case equivalent permittivity of the air and paper combination). The second part of the inductance takes into account the flux internal to the conductor [6]. It is given by:

$$L_i = \frac{R}{f} \quad (14)$$

where R is from the real part of (7) and f is the frequency. The total inductance matrix can be expressed as:

$$L = L_n + L_i \cdot E_n \quad (15)$$

where E_n is a unit matrix of size $n \times n$. It should be noted that the MTL model has also been applied for a disc winding in [22].

VI. MEASUREMENTS AND SIMULATIONS

A. Test Equipment

The equipment used included a Krohn-Hite Power Amplifier 7602 M series, 20 MHz Agilent 3320A waveform generator and Tektronix DPO 3032 Oscilloscope 300 MHz, 2.5 GS/s.

The power amplifier is connected after the signal generator to keep the input voltage fairly constant. The amplifier energizes the whole winding whilst the oscilloscope measures the layer voltages from the measuring taps shown in Fig. 3 as the output. The RVR ratio was used to ascertain if resonance had occurred or not.

B. Comparison of measured and calculated results

As previously mentioned, resonance can be classified as either internal or external resonance. It is worth noting that internal resonance can be further defined as internal voltage maximum and internal anti-resonance as internal voltage minimum [23]. This relationship will be crucial in the analysis of measured and calculated results. Comparison will not be done for all 16 layers, however only crucial results will be revealed in this paper. In Figs. 5, 6 and 7 it can be seen that there is a relatively good agreement between the calculated and measured results.

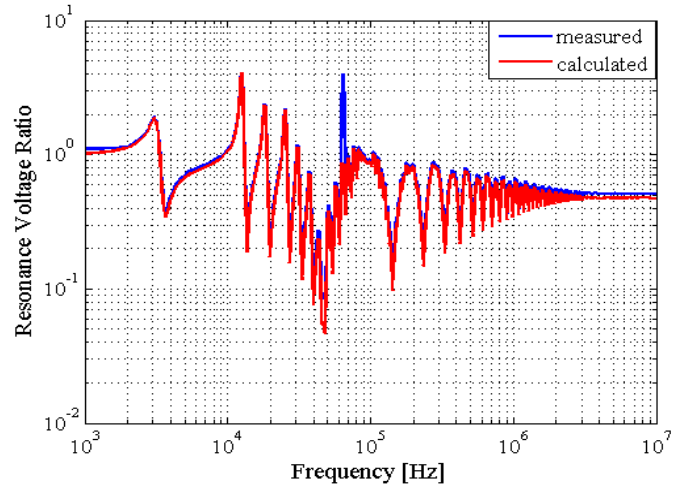


Fig. 5. Resonance voltage ratio across layer 1 – measured (across lead 1 and 2 in Fig. 3) vs calculated.

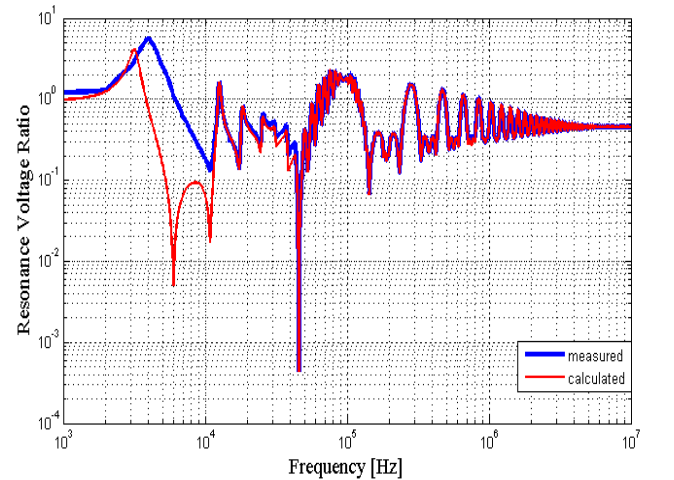


Fig. 6. Resonance voltage ratio across layer 15 – measured (across lead 15 and 16 in Fig. 3) vs calculated.

The calculated results follow the profile of the measured results although there is a frequency shift between 1 kHz and 10 kHz for layers 15 and layer 16. The general trend of the

resonance voltage ratio is shown in Fig. 8, 9, 10 and 11.

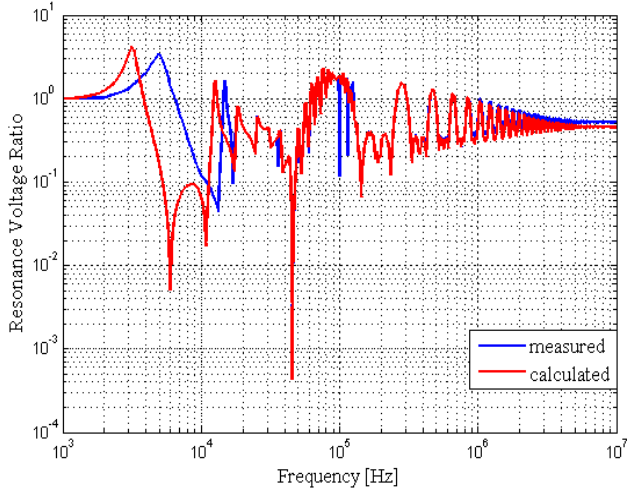


Fig. 7. Resonance voltage ratio across layer 16 – measured (across lead 16 and 17 in Fig. 3) vs calculated.

layer 5. Then the magnitude starts to decrease for layers 9 to layer 16.

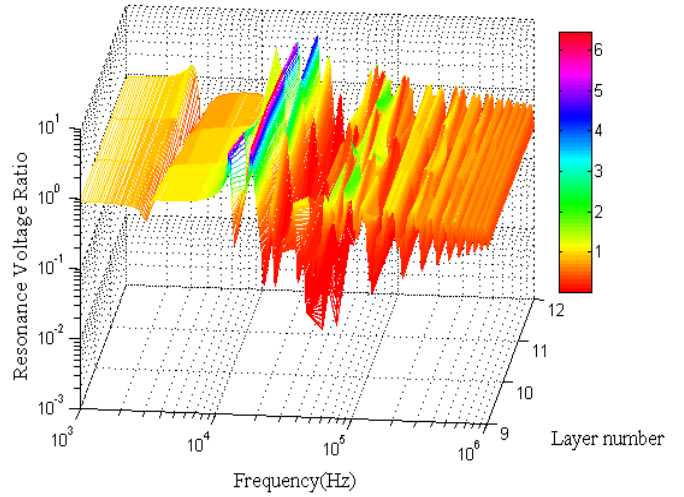


Fig. 10. Measured: resonance voltage distribution in layers 9-12.

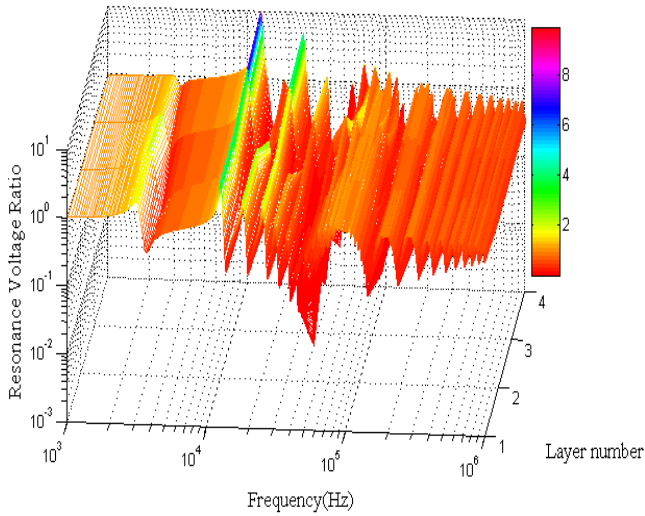


Fig. 8. Measured: resonance voltage distribution in layers 1-4.

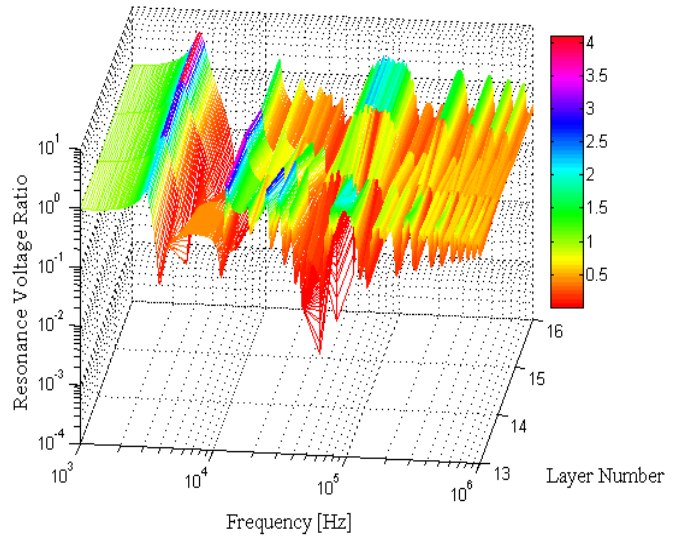


Fig. 11. Measured: resonance voltage distribution in layers 13-16.

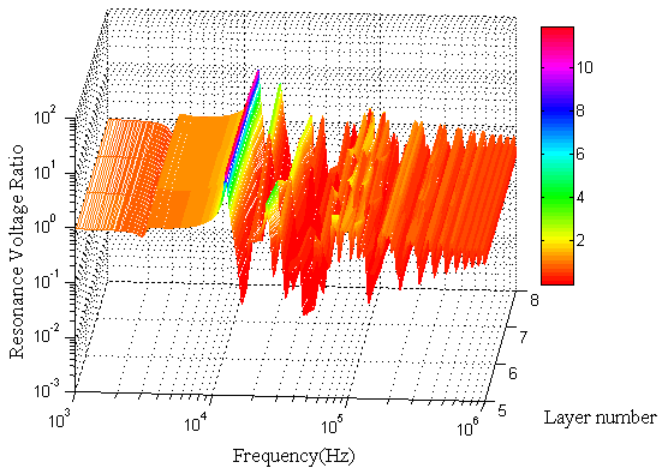


Fig. 9. Measured: resonance voltage distribution in layers 5-8.

It is interesting to note that the magnitude of the resonant overvoltages increase as you approach the break i.e. layer 1 to

VII. SWITCHING SURGE MEASUREMENT AND ANALYSIS

As previously mentioned, internal resonance occurs when a frequency component of the incoming surge equals a resonant frequency of the transformer leading to resonant overvoltages. In order to investigate the impact of switching surges in the development of resonant overvoltages the following tests were performed:

1. Energizing the transformer during no-load.
2. Disconnecting the transformer during no-load.

Measurement of the three MV phase-to-earth voltages was done using a capacitive voltage divider on each phase. The MV bushing screen had a measured capacitance of 32 pF and an additional capacitance of 10 nF was externally mounted in series with the bushing screen terminal and the transformer tank which provided local earth. The resulting voltage division ratio was 313.

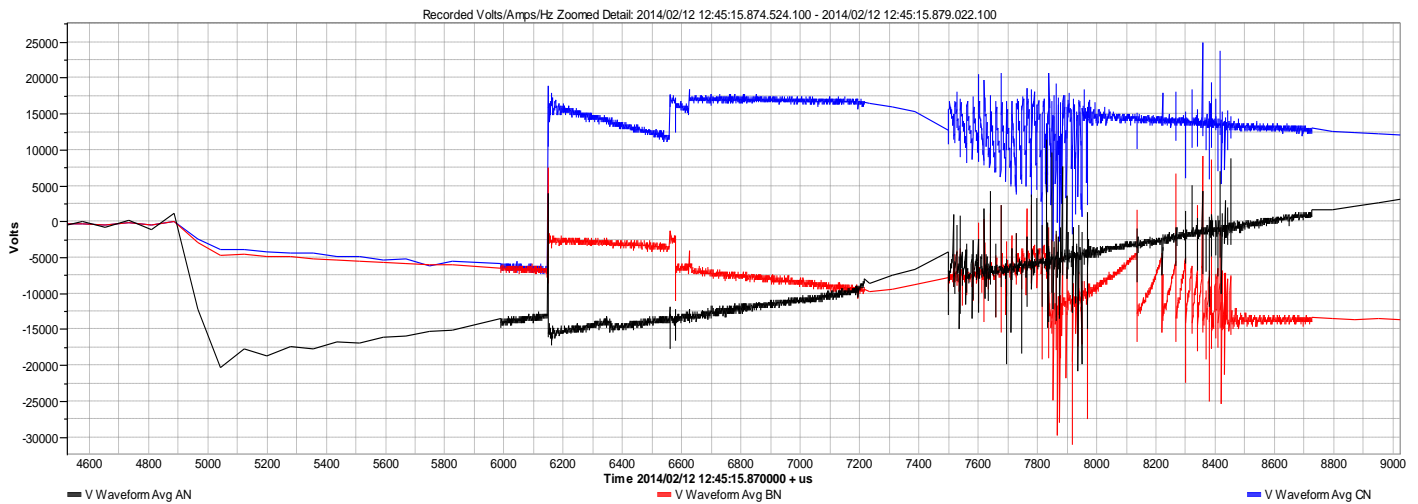


Fig. 13. Measured pre-strikes which show a high du/dt

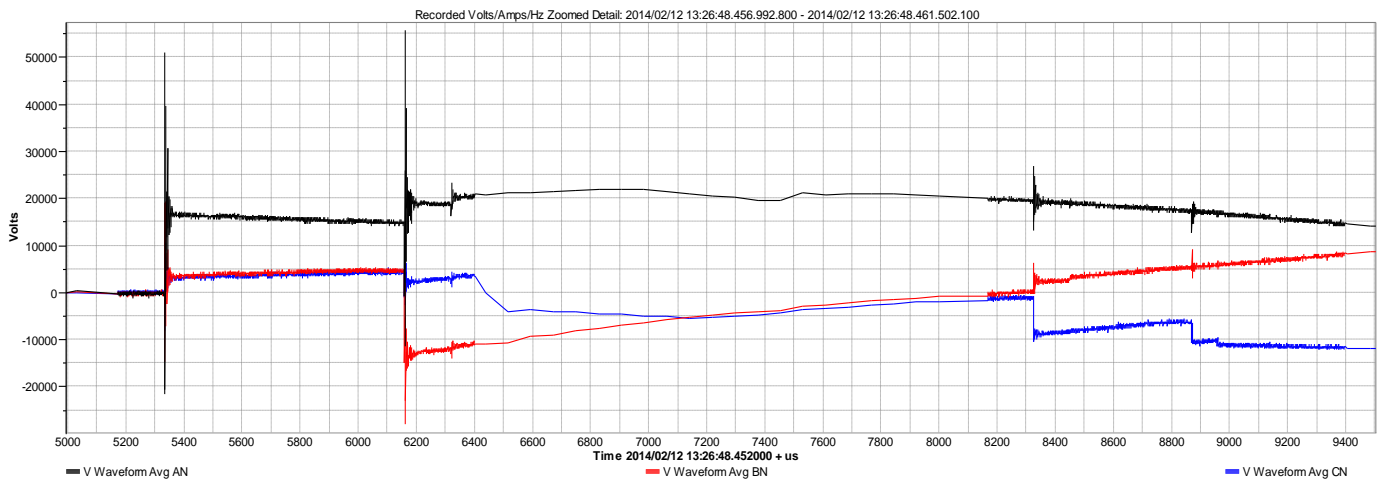


Fig. 14. Measured pre-strikes which show a high du/dt

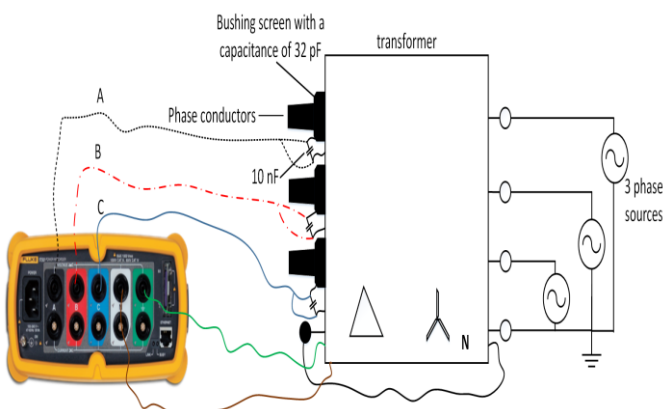


Fig. 12. Measurement setup for recording transient events during switching.

The setup for recording the transient events is shown in Fig. 12. It should be noted that the above setup measures phase to earth voltages on the MV side. Measurement of the voltage waveforms was done using a Fluke 1750 Power Recorder which samples transients at 5 Mega samples per second.

A. Energizing the transformer during no-load

Energization of the transformer always results in at least one pre-strike per phase [24]. During the contact making process of the vacuum circuit breaker, generation of high du/dt transients can occur at the transformer terminals leading to over-voltages [7]. This behaviour can be observed from the measured transients in Figs. 13 and 14. Analysis of the measured waveforms show that there is substantial overshoot and ringing when the contacts are closed. Also from Figure 14, the peak value of the second peak is almost 2.5 times above the system voltage. Since relatively short cables of small surge impedance exist between the VCB and the transformer, this type of low surge impedance connection has a low du/dt limiting effectiveness [7]. Hence the high value of overvoltages and high frequency transients which were measured.

B. De-energizing the transformer during no-load

On disconnection by the VCB higher over-voltages can occur if the arc re-ignites after the first current interruption [25]. If the VCB is not able to quench the arc, multiple re-ignitions can occur and with each re-ignition, the voltage escalates

resulting in higher overvoltages. No significant over-voltages were measured on de-energizing of the transformer.

VIII. DISCUSSION

In [26], research was conducted on the performance of oil impregnated cellulose paper when subjected to transients with different repetition frequency, rise time and magnitude. It was found that the faster the rise time, the more damage to the insulation that occurs and the quicker the transient reaches its peak value the more profound the damage to the insulation. Most commonly used insulation paper in transformers is Krempel DPP 0.25mm which has a breakdown voltage in oil of 13.5 kV [27]. From the peak values in Figs. 13 and 14, it is possible to design the insulation system such that it is able to withstand the high overvoltages between the layers. However the repetition rate would require damping by series connected choke elements [7]. It should be noted that the insulation system of the wound core transformer withstood the routine induced overvoltage test specified in IEC 60076 and complied with the impulse test in IEC 60076.

Use of the MTL model was possible since precise design information was made available by the transformer manufacturer. However no tan (δ) testing is done for an MV distribution transformers hence an approximated equation was used. As previously mentioned equation (9) will not take into account the detailed frequency dependency of the dissipation factors of the transformer insulation, which are crucial for accurate modelling using the MTL model. This could explain why the model was not able to accurately predict certain resonance frequencies for the transformer winding.

Two transformer designs have been presented. The major difference is the transformer with the split winding has higher resonant overvoltages below 100 kHz whereas the investigated transformer that had a non-split winding had high resonant overvoltages above 500 kHz. The split winding could be the reason why only the top half of the coil participates in resonances as can be seen by the decreasing trend of the resonant voltage ratio in Figs. 8, 9, 10 and 11.

Although the two transformers also differed in the type of core used, where the failed transformer used a wound core as opposed to the constructed prototype which used a stacked core, the focus was on resonance performance between a split MV winding versus a non-split MV winding. Customers usually prefer a transformer with a stacked core over the wound core. This is largely due to difficulties associated with a wound core when compared to a stacked core which are [28] (i) air gaps may diverge due to the tolerances of the machine during the cutting and winding of the sheets and also difficulties in processing of the magnetic material (ii) obtaining accurate dimensions in stacked cores is much easier than in wound cores during cutting (iii) core formation may deteriorate the magnetic material insulation and (iv) homogeneous temperature distribution in a wound core is hard to obtain during the annealing procedure as compared to stacked cores.

The measurement of resonance voltage ratio in this paper was done using the oscilloscope and signal generator. These measured RVR were needed for comparison with the

calculated RVR in equation (6) for resonance analysis. However a different technique could have been done using frequency response analysis equipment where the impedance characteristics of the winding are determined. Both analysis techniques have been shown to produce the same results as shown in [29].

IX. CONCLUSION

In this paper, resonance phenomena in transformer windings and the measurement of switching transients have been presented. The MTL model has been used to calculate the magnitude of the resonant overvoltages within the layers and to determine between which layers breakdown could occur. Different winding designs were also investigated and their effect on part winding resonance was explored. The developed model still has several shortcomings; however it can be used in the prediction of resonances, especially in layer type transformers.

X. ACKNOWLEDGMENT

The author would like to thank the engineers from the transformer factory and the wind farm for allowing us to do measurements and research on different transformer designs.

XI. REFERENCES

- [1] T. Craenenbroek, J. D. Ceuster, J. P. Marly, H. D. Herdt, B. Brouwers, and D. V. Dommelen. "Experimental and numerical analysis of fast transient phenomena in distribution transformers." in *IEEE Power Engineering Society Winter Meeting, Singapore*, vol. 3, no. 1, pp. 2193–2198, Jan. 2000.
- [2] M. Popov and L. van der Sluis. "Improved calculations for no-load transformer switching surges." in *IEEE Transactions on Power Delivery*, vol. 16, no. 3, pp. 401–408, Jan. 2001.
- [3] A. H. Soloot, H. K. Hodalen, and B. Gustavsen. "Modeling of Wind Turbine Transformers for the Analysis of Resonant Overvoltages." in *International Conference on Power Systems Transients IPST2013 in Vancouver, Canada*, pp. 1–7, Jul. 2013.
- [4] M. Popov, L. V. der Sluis, G. C. Paap, and H. D. Herdt. "Computation of Very Fast Transient Overvoltages in Transformer Windings." in *IEEE Transactions on POWER DELIVERY*, vol. 18, no. 4, pp. 1268–1274, Oct. 2003.
- [5] H. Sun, G. Liang, X. Zhang, and X. Cui. "Analysis of Resonance in Transformer Windings under Very Fast Transient Overvoltages." in *17th International Zurich Symposium on Electromagnetic Compatibility*, vol. 22, no. 1, pp. 432–435, Jan. 2006.
- [6] H. Sun, G. Liang, X. Zhang, and X. Cui. "Modelling of Transformer Windings under Very Fast Transient Overvoltages." in *IEEE Transactions on Electromagnetic Compatibility*, vol. 48, no. 4, pp. 621–627, Nov. 2006.
- [7] D. Smugala, W. Piasecki, M. Ostrogorska, M. Florkowski, M. Fulczyk, and P. Kyles. "Distribution transformers protection against High Switching Transients." *Przegląd Elektrotechniczny (Electrical Review)*, pp. 296 – 300, Jan. 2012.
- [8] CIGRE. "Electrical Transient Interaction between Transformers and the POWER SYSTEM." In *PART 1: EXPERTISE by CIGRE Joint Working Group A2/C4.39, Chapter. 4: Transformer Modelling*, CIGRE ISBN: 978-2-85873272-2, pp. 33–56. Apr. 2014.
- [9] R. Asano, A. C. O. Rocha, and G. M. Bastos. "Electrical transient interaction between transformers and the power system." in *CIGRE-33 CIGRE Brazil JWG A2/C4-03*, pp. 401–408, Jun. 2007.
- [10] A. C. O. Rocha. "Electrical transient interaction between transformers and the power system." in *CIGRE C4-104, CIGRE Brazil JWG A2/C4-*

- 03, Paris, France, pp. 1–7, Jun. 2008.
- [11] A. Theocharis, M. Popov, R. Seibold, S. Voss, and M. Eiselt. “Analysis of Switching effects of Vacuum Circuit Breaker on *Dry-Type* Foil winding transformers validated by experiments.” in *IEEE Transactions on Power Delivery*, pp. 1–9, May 2014.
- [12] A. H. Soloot, H. K. Hodalen, and B. Gustavsen. “Upon the Improvement of the Winding Design of Wind Turbine Transformers for Safer Performance within Resonance Overvoltages.” in *proc. of CIGRE Joint Colloquium - SC A2/C4*, pp. 1–7, 2013.
- [13] A. H. Soloot, H. K. Hodalen, and B. Gustavsen. “The effect of winding design on transformer frequency response with application on offshore wind farm energization.” in *proc. Of Intl. Conference on Renewable Energy Research and Applications (ICRERA)*, pp. 1–7, Nov. 2012.
- [14] A. H. Soloot, H. K. HÅidalen, and B. Gustavsen. “Internal Resonant Overvoltage in Wind Turbine Transformers- Sensitivity Analysis of Measurement Techniques.” in *International Conference on Electrical Machines and Systems, Busan, Korea*, pp. 1–7, Oct. 2013.
- [15] M. Popov, L. V. der Sluis, R. P. P. Smeets, and J. L. Roldan. “Analysis of Very Fast Transients in *Layer-Type* Transformer Windings.” in *IEEE TRANSACTIONS ON POWER DELIVERY*, vol. 22, no. 1, pp. 238–247, Jan. 2007.
- [16] M. Popov, L. V. der Sluis, and R. P. P. Smeets. “Evaluation of surge-transferred overvoltages in distribution transformers.” in *Electric Power Systems Research 78 (ELSEVIER)*, vol. 78, no. 3, pp. 441–449, May 2007.
- [17] J. Guardado and K. J. Cornick. “A Computer model for calculating Steep-Fronted Surge Distribution in Machine Windings.” in *IEEE TRANSACTIONS ON Energy Conversion*, vol. 4, no. 1, pp. 95–101, Mar. 1989.
- [18] J. A. Martinez-Velasco. “Power System Transients.” In *Parameter Determination, Chapter 4: Transformers*, CRC Press Taylor and Francis Group, ISBN 978-1-4200-6529-9 (Hardback), pp. 177–255. 2010.
- [19] Y. Shibuya, S. Fujita, and N. Hosokawa. “Analysis of very fast transient overvoltage in transformer winding.” in *IEE Proc.-Gener. Transm. Distrib*, vol. 144, no. 5, pp. 461–468, 1997.
- [20] F. de Leon and A. Semlyen. “Reduced order model for transformer transients.” in *IEEE Transactions on Power Delivery*, vol. 7, no. 1, pp. 361–369, Jan. 1992.
- [21] F. de Leon and A. Semlyen. “Efficient calculation of Elementary parameters of Transformer.” in *IEEE Transactions on Power Delivery*, vol. 7, no. 1, pp. 376–383, Jan. 1992.
- [22] C. A. Banda and J. M. Van Coller, “Measurement of switching surges and resonance behavior in transformer windings,” in *Proceedings of the 23rd Southern African Universities Power Engineering Conference*, pp. 496-501. Jan 2015.
- [23] R. C. Degeneff. “A general method for determining resonances in transformer windings.” in *IEEE Transactions on Power Apparatus and Systems*, vol. PAS-96, no. 2, pp. 423–430, Mar. 1977.
- [24] L. Liljestrand, E. Lindell, D. Bormann, C. Ray, and E. Dullni. “Vacuum circuit breaker and Transformer interaction in a cable system.” *CIREC 22nd International Conference on Electricity Distribution Stockholm*, no. 0412, pp. 1–4, Jun. 2013.
- [25] A. Mueller and D. Saemann. “Switching phenomena in Medium Voltage Systems - Good Engineering Practise on the application of Vacuum circuit breakers and contractors.” pp. 1–9, Mar. 2011.
- [26] T. L. Koltunowicz, R. Kochetov, G. Bajracharya, D. Djairam and J. J. Smit “Repetitive Transient Aging, the Influence of Rise Time” in *Electrical Insulation Conference, Annapolis, Maryland* pp.151-155, Jun 2011
- [27] KREMPEL, “Technical datasheet KREMPEL DPP.” P. 11/96 Aug. 2012
- [28] P.S. Georgilakis, N.D. Hatziaargyriou, N.D. Doulamis, A.D. Doulamis and S.D. Kollias, “Prediction of iron losses of wound core distribution transformers based on artificial neural networks” in *Neurocomputing 23 (ELSEVIER)*, pp. 15-29, July 1998.
- [29] IEEE, “Guide to describe the occurrence and mitigation of switching transients induced by transformers, switching device, and system interaction,” *IEEE Std C57.142*, pp. 35, Dec. 2010.